ARTICLE

Postglacial viability and colonization in North America's ice–free corridor

Mikkel W. Pedersen[1], Anthony Ruter[1], Charles Schweger[2], Harvey Friebe[2], Richard A. Staff[3], Kristian K. Kjeldsen[1,4], Marie L. Z. Mendoza[1], Alwynne B. Beaudoin[5], Cynthia Zutter[6], Nicolaj K. Larsen[1,7], Ben A. Potter[8], Rasmus Nielsen[1,9,10], Rebecca A. Rainville[11], Ludovic Orlando[1], David J. Meltzer[1,12], Kurt H. Kjær[1] & Eske Willerslev[1,13,14]

During the Last Glacial Maximum, continental ice sheets isolated Beringia (northeast Siberia and northwest North America) from unglaciated North America. By around 15 to 14 thousand calibrated radiocarbon years before present (cal. kyr BP), glacial retreat opened an approximately 1,500–km–long corridor between the ice sheets. It remains unclear when plants and animals colonized this corridor and it became biologically viable for human migration. We obtained radiocarbon dates, pollen, macrofossils and metagenomic DNA from lake sediment cores in a bottleneck portion of the corridor. We find evidence of steppe vegetation, bison and mammoth by approximately 12.6 cal. kyr BP, followed by open forest, with evidence of moose and elk at about 11.5 cal. kyr BP, and boreal forest approximately 10 cal. kyr BP. Our findings reveal that the first Americans, whether Clovis or earlier groups in unglaciated North America before 12.6 cal. kyr BP, are unlikely to have travelled by this route into the Americas. However, later groups may have used this north–south passageway.

Understanding the postglacial emergence of an unglaciated and biologically viable corridor between the retreating Cordilleran and Laurentide ice sheets is a key part of the debate on human colonization of the Americas[1–3]. The opening of the ice-free corridor, long considered the sole entry route for the first Americans, closely precedes the 'abrupt appearance' of Clovis, the earliest widespread archaeological complex south of the ice sheets at ~13.4 cal. kyr BP[4,5]. This view has been challenged by recent archaeological evidence that suggests people were in the Americas by at least 14.7 cal. kyr BP[6,7], and possibly several millennia earlier[8]. Whether this earlier presence relates to Clovis groups remains debated[9]. Regardless, as it predates all but the oldest estimates for the opening of the ice-free corridor[10,11], archaeological attention has shifted to the Pacific coast as an alternative early entry route into the Americas[1,11]. Yet, the possibility of a later entry in Clovis times through an interior ice-free corridor remains open[1,9,12].

Whether the ice-free corridor could have been used for a Clovis-age migration depends on when it became biologically viable. However, determining this has proven difficult because radiocarbon and luminescence dating of ice retreat yield conflicting estimates for when the corridor opened, precluding precise reconstruction of deglaciation chronology[10,13–17]. Once the landscape was free of ice and meltwater, it was open for occupation by plants and animals, including those necessary for human subsistence. On the basis of studies on modern glaciers[18], the onset of biological viability could have been brief (for example, a few decades) if propagules were available in adjacent areas, and assuming they were capable of colonizing what would have been a base-rich (high pH) and nitrogen-poor, soil substrate (such as nitrogen-fixing plants like *Shepherdia canadensis* (buffaloberry)).

Establishment of biota within the corridor region must have varied locally depending on the rate and geometry of ice retreat, the extent of landscape flooding under meltwater lakes, and the proximity of plant and animal taxa and their dispersal mechanisms[1,19,20]. Some areas were habitable long before others. Although the corridor's deglaciation history was complex, broadly speaking it first opened from its southern and northern ends, leaving a central bottleneck that extended from approximately 55 °N to 60 °N[1,10,13–15,21]. On the basis of currently available geological evidence, this was the last segment to become ice free and re-colonized by plants and animals[1,13,22–24].

Although palynological and palaeontological data can be used to help study the opening of the corridor region, these are limited in several respects. First, not all vegetation, particularly pioneering forbs and shrubs, produce pollen and macrofossils with good preservation potential that will be detectable in available depositional locales. Hence, timing of plants' appearance may be underestimated. Second, pollen can disperse over long distances and have limited taxonomic resolution, differential preservation, and variable production rates, all of which can bias vegetation reconstruction[25]. Third, fossil evidence for initial large mammal populations that dispersed into the newly opened corridor is sparse. The fossil remains suggest the presence of bison, horse and mammoth, and probably some camel, muskox and caribou[26,27]. Yet, the oldest vertebrate remains after the Last Glacial Maximum are no older than ~13.5 cal. kyr BP[2], and those specimens are found outside the bottleneck region[1,3,26,28,29]. These animals would have been the source populations to recolonize the newly opened landscape, and thus their presence within the bottleneck region can indicate when the corridor became a viable passageway over its entirety.

Samples and analytical approaches

To overcome current limitations of the palaeoecological record, and develop a more precise chronology for the opening and biological viability of corridor's bottleneck region, we collected nine lake sediment cores from Charlie Lake and Spring Lake in the Peace River drainage

[1]Centre for GeoGenetics, Natural History Museum, University of Copenhagen, Copenhagen 1350, Denmark. [2]Department of Anthropology, University of Alberta, Edmonton, Alberta T6G 2H4, Canada. [3]School of Archaeology, University of Oxford, Oxford OX1 3QY, UK. [4]Department of Earth Sciences, University of Ottawa, Ottawa, Ontario K1N 6N5, Canada. [5]Royal Alberta Museum, Edmonton, Alberta T5N 0M6, Canada. [6]Department of Anthropology, MacEwan University, Edmonton, Alberta T5J 4S2, Canada. [7]Department of Geoscience, Aarhus University, 8000 Aarhus, Denmark. [8]Department of Anthropology, University of Alaska Fairbanks, Fairbanks, Alaska 99775, USA. [9]Department of Integrative Biology, University of California, Berkeley, California 94720-3140, USA. [10]Department of Biology, University of Copenhagen, 2200 Copenhagen, Denmark. [11]Department of Archaeology, University of Calgary, Calgary, Alberta T2N 1N4, Canada. [12]Department of Anthropology, Southern Methodist University, Dallas, Texas 75275, USA. [13]Department of Zoology, University of Cambridge, Cambridge CB2 3EJ, UK. [14]Wellcome Trust Sanger Institute, Cambridge CB10 1SA, UK.
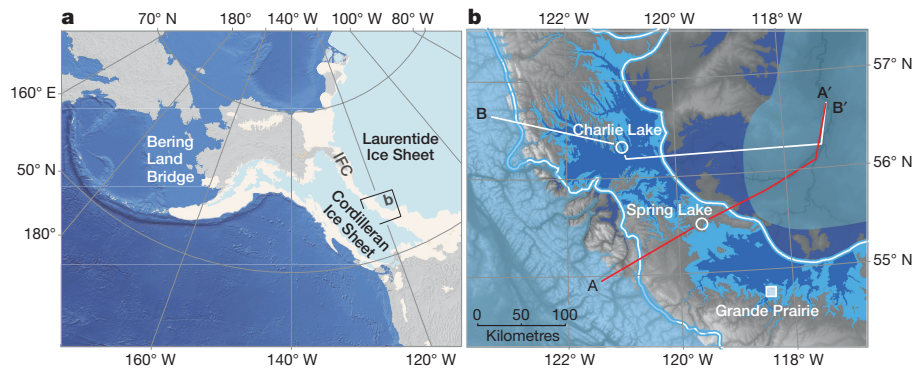
Figure 1 | Setting and study area. During the Last Glacial Maximum, the Laurentide Ice Sheet and the Cordilleran Ice Sheet coalesced in western mid-Canada creating a physical barrier to north–south migration. Following the Last Glacial Maximum, the ice retreated creating an ice-free corridor (IFC). **a**, Ice extent[10] during two periods, Last Glacial Maximum 21.4 cal. kyr BP (off-white) and Late Pleistocene 14.1 cal. kyr BP (light-blue).

b, Topography of the Peace River basin with Glacial Lake Peace Phase III (white lines with blue outlines) and Phase IV[13] with ice extent[10] (light-blue and dark-blue) at around 14.1 cal. kyr BP and 13 cal. kyr BP, respectively. The red and white lines mark topographic transects of the lakes which in relation to the four phases of Glacial Lake Peace[13] is found in Extended Data Fig. 1.

basin (Fig. 1). These are remnants of Glacial Lake Peace, which formed as the Laurentide Ice Sheet began to retreat in this region around 15 to 13.5 cal. kyr BP and blocked eastward draining rivers[10,13–15,21] (Extended Data Fig. 1). Glacial Lake Peace flooded the gap between the ice fronts until about 13 cal. kyr BP, sometime after which Charlie and Spring lakes became isolated[13]. Thus, this area was amongst the last segments of the corridor to open and is pivotal to understanding its history as a biogeographic passageway[1,13,14,16,22,24].

Of the nine cores obtained from Charlie Lake and Spring Lake, one from each lake predates the Pleistocene to Holocene transition, the oldest dating to ~12.9 cal. kyr BP (modelled age). We sampled the cores from both lakes for magnetic susceptibility, pollen[30,31], micro- and macrofossils, including ^{14}C-dateable material for subsequent robust Bayesian age-depth modelling (Fig. 2, Methods, Extended Data Figs 2–4 and Supplementary Information). In addition, we obtained environmental DNA (eDNA)[32], representing molecular fossils of local organisms derived from somatic tissues, urine and faeces[33], but rarely pollen[34]. eDNA complements traditional pollen and macrofossil studies[35], and is especially useful for establishing the likelihood that a taxon occurred within a particular time period[36,37]. Furthermore, eDNA enables identification of taxa even in the absence of micro- and macrofossil material, thus improving the resolution of taxonomic richness surveys[36]. However, amplification of short and taxonom- ically informative DNA metabarcodes[38] can be biased towards taxa targeting[35]. We used shotgun sequencing of the full metagenome in the DNA extracts to reveal the whole diversity of taxonomic groups present in the sediment[39] (Fig. 2, Methods, Extended Data Figs 5 and 6 and Supplementary Information). We confirmed the sequences identified as ancient by quantifying DNA damage[40], and found the DNA damage levels to accumulate with age (Pearson correlation coefficient = 0.663, P value = 0.00012) (Methods and Extended Data Fig. 7a, b).

Biological succession within the corridor bottleneck

The basal deposit in the Charlie Lake core is proglacial gravel, previously reported from the area[22], above which are laminated lacustrine sediments, principally composed of silt-sized grains[24] (Extended Data Fig. 2). We interpret these as deposits from Glacial Lake Peace Stage IV (ref. 13), the >15,000 km² proglacial lake that covered the Peace River area of northeastern British Columbia and northwest- ern Alberta. A subsequent lithological change from silt to sandy organic rich mud (gyttja) at the onset of Holocene, around 11.6 cal. kyr BP, reflects a change in sediment source and lake productivity we interpret as Charlie Lake becoming isolated from Glacial Lake Peace (Fig. 1). This is followed by a decrease in pollen influx in both lake records at ~11.5 cal. kyr BP that coincides with an increase in pre-Quaternary palynomorphs. At Charlie Lake there is then a marked increase in
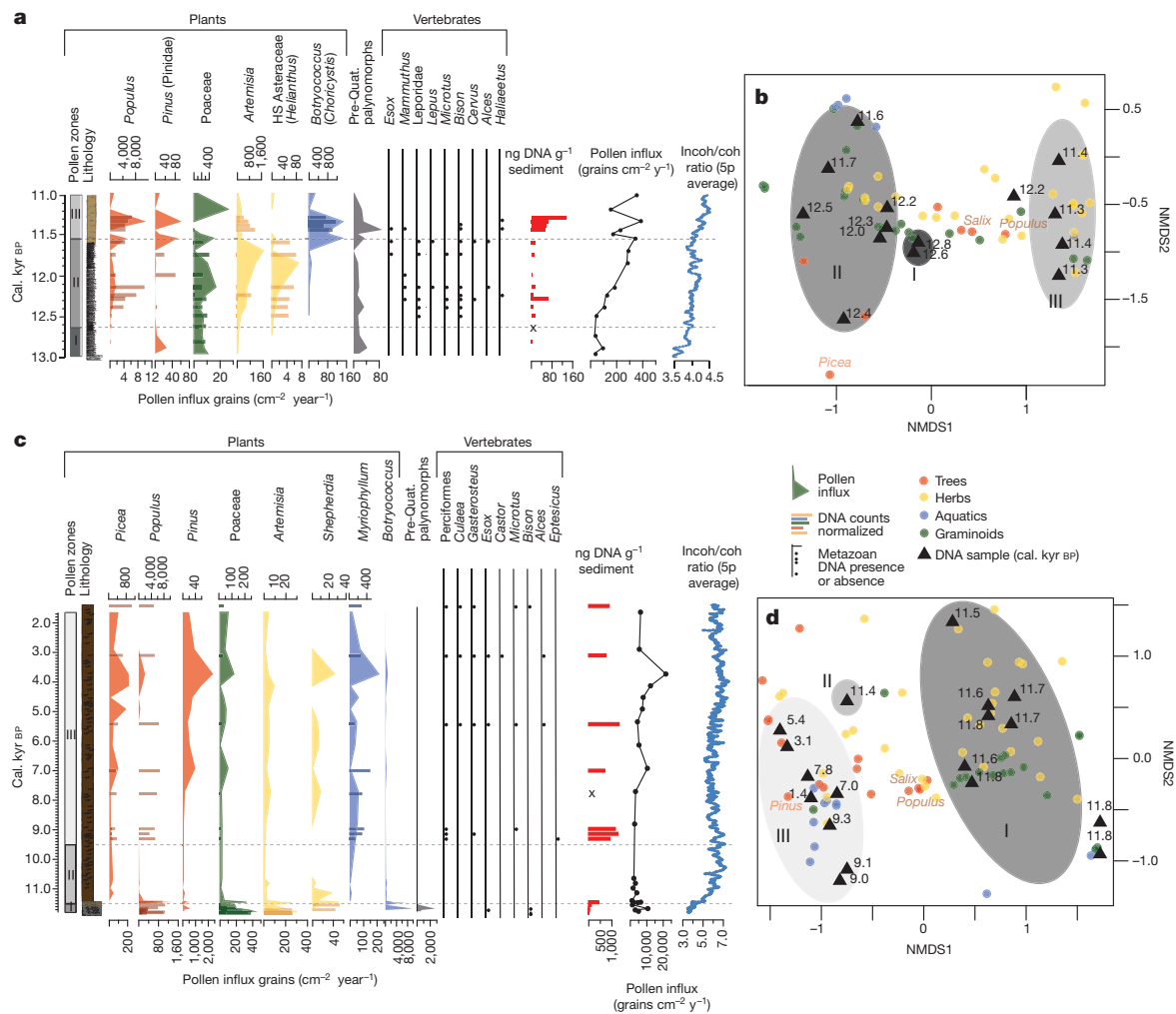
pollen influx at ~11.3 cal. kyr BP. We interpret these fluctuations as responses of a highly dynamic landscape to paraglacial and aeolian redepositional processes.

Our palynological and eDNA-based taxonomic identifications, respectively, reveal the development of biota in the regional and local environment surrounding each lake (Fig. 2, Extended Data Figs 3–6). Prior to ~12.6 cal. kyr BP (Charlie Lake, pollen zone I, ~13 to 12.6 cal. kyr BP), the bottleneck area appears to have been largely unvegetated, receiving low pollen influx (<50 grains cm^{-2} y^{-1}) with little organic content (incoherent/coherent ratio) and low DNA concentrations (<5 ng per g of sediment). During the later phases of Glacial Lake Peace, both pollen and eDNA indicate grasses and sedges were early colonizers. Charlie Lake pollen zone II (~12.6 to 11.6 cal. kyr BP) contains evidence of steppe vegetation, including *Artemisia* (sagebrush), Asteraceae (sunflower family), Ranunculaceae (buttercup family), Rosaceae (rose family, rosids in eDNA), *Betula* (birch), and *Salix* (willow). A similar plant community is recorded at Spring Lake (pollen zone 1), with substantial abundances of *Populus* and *S. canadensis*, probably due to elevation differences and because by this time Spring Lake was no longer part of the Glacial Lake Peace system.

eDNA indicates the steppe vegetation supported a variety of animals including *Bison* which appear at ~12.5 cal. kyr BP, and *Microtus* (vole) and *Lepus* (jackrabbit) by ~12.4 cal. kyr BP (Fig. 3). After 12.4 cal. kyr BP, *Populus* trees became more dominant and *Cervus* (elk), *Haliaeetus* (bald eagle) and *Alces* (moose) appear in the eDNA record. The productivity of the bottleneck increased to a peak at ~11.6 cal. kyr BP. The presence of *Esox* (pike), a top aquatic predator, implies that by ~11.7 cal. kyr BP, a fish community was already established. After 11.6 cal. kyr BP, *Picea* (spruce), *Pinus* (pine) and *Betula* pollen increased in the Charlie Lake pollen record, reflecting the establishment of boreal forest.

Around 11.5 cal. kyr BP, a distinct decline occurred in pollen influx at both lakes. High abundance of *Botryococcus* (green algae) in each is probably a response to changing nutrient sources, lake chemistry, sediment input and possibly reduced turbidity following isolation of these basins from Glacial Lake Peace[41]. *Botryococcus* dominated the early Holocene sequence in Spring Lake (11.7–11.5 cal. kyr BP) but declined relative to *Pediastrum* (green algae) after 11.0 cal. kyr BP, consistent with eutrophication in a more productive ecosystem. Pollen and plant macrofossils indicate *Alnus* (alder) was in the vicinity of Spring Lake at about 7.0 cal. kyr BP, although it is not evident in eDNA until approximately 5.5 cal. kyr BP.

We used non-metric multi-dimensional scaling (NMDS) based on Bray–Curtis similarity measures to explore whether the eDNA plant communities, excluding algae, reflect the pollen data (Fig. 2b, d).
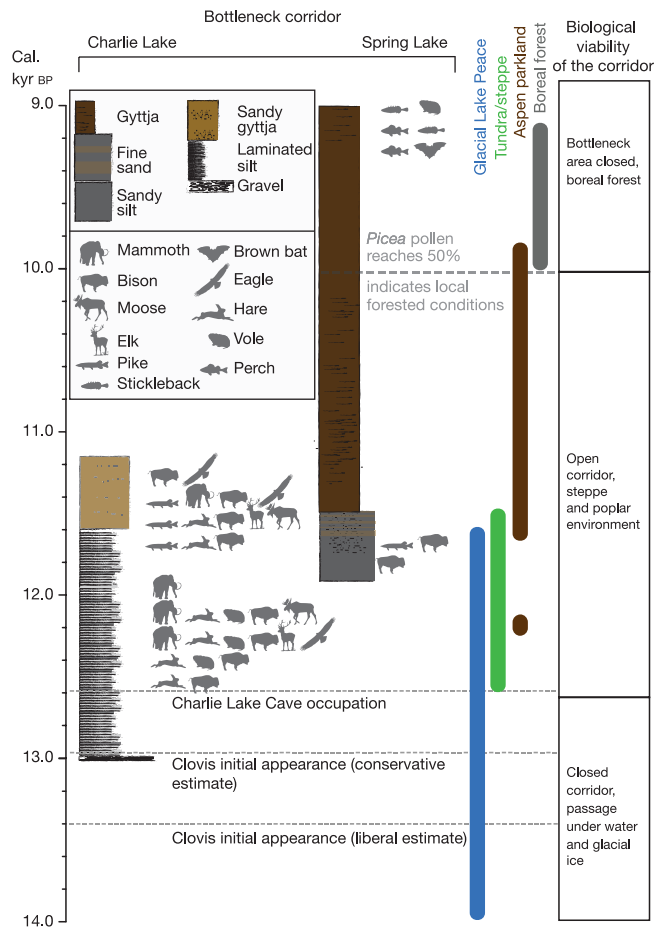
Figure 2 | Selected pollen, DNA and biometrical results. a, **c**, Pollen are presented as influx (area) and DNA taxa presented with normalized counts (bars). HS asteraceae, high spike asteraceae. Metazoans are presented with bullet points indicating their presence. The 5 point average (5p) of the incoherent/coherent (incoh/coh) ratio is derived from the X-ray fluorescence results and an increasing ratio represents increased organic content. **b**, **d**, Non-metric multi-dimensional scaling plots; grey ellipses marked I, II, and III encircle the samples corresponding to the respective CONIIC pollen zonation. Coloured dots indicate each taxon identified. The coloured categories are identical to the pollen and DNA taxa in Charlie Lake (**a**), and Spring Lake (**c**).

In eDNA samples, the first NMDS axis matches the clear separation between major pollen zones at Spring Lake and Charlie Lake. The only exception is represented by the 12.2 cal. kyr BP sample at Charlie Lake, which does not cluster with other samples of similar age (~12.6–11.6 cal. kyr BP) but is closer to the arboreal and younger samples from pollen zone I. Nevertheless, consistency between the main pollen zones and clustering of eDNA samples confirms that large ecological changes found in pollen records can be identified using eDNA.

Despite good conformity between palynological and eDNA data, some discrepancies suggest these proxies are variably affected by a plant's reproductive process and taphonomic history (see Supplementary Information). The most notable of these discrepancies is the *Populus* record. In Charlie Lake, its pollen and eDNA signals are congruent from ~11.6–11.2 cal. kyr BP, whereas earlier (~12.4–12.1 cal. kyr BP) the eDNA signal for *Populus* is more pronounced. In Spring Lake, *Populus* pollen only occurs towards the base of the record and in upper zone III, whereas in the eDNA record it is abundant throughout. This discrepancy is probably due to *Populus* reproducing vegetatively, and its notoriously low detection rates and poor pollen preservation, which often render it palynologically 'silent'[42]. The eDNA reveals that poplar was probably more abundant in the regional vegetation than has previously been shown with palynology. This has important implications for human occupation as poplar would

have provided wood for fuel, shelter, and tools, as well as browse feeding for animals.

The differences between the pollen and eDNA evidence for plants might also reflect dispersal factors. Wind-dispersed pollen is more likely to be encountered in lake-based pollen records, whereas predominantly insect-pollinated taxa are less likely to settle in lake sediments and be detected. Many willows (*Salix* spp.), for example, are insect pollinated. Their pollen is present in low percentage (5%) in zone II in Charlie Lake, but in higher abundance in zones II and III in the eDNA record (Extended Data Figs 5 and 6). This suggests the eDNA comes more from macrofossils and plant debris than from pollen.

The eDNA record also detects taxa not present in fossil bone assemblages, including terrestrial and aquatic vertebrates. In particular, it identifies top-level aquatic (*Esox*) and avian (*Haliaeetus*) predators, which indicate a rich supporting community at lower trophic levels. *Cervus* is evident in the Charlie Lake record at about 11.5 cal. kyr BP, whereas its earliest fossil remains from the area date to about 10.2 cal. kyr BP[43]. Small mammals, such as *Microtus* are documented in the Charlie Lake eDNA at 12.4 cal. kyr BP confirming the *Microtus* colony found just west of Charlie Lake, at Bear Flats[43]. Yet, there are also notable absences in eDNA compared to the vertebrate record. For example, faunal remains from the adjacent Charlie Lake Cave, dated to ~12.4 cal. kyr BP[44] are rich in waterfowl and other birds and fish not

Figure 3 | Ecological interpretation and implications of this study.
Timeline of the biology in the bottleneck area linking it with evidence of human occupation and the first appearance of Clovis technology (see also Fig. 4). Grey animal silhouettes are vertebrate genera that were identified by environmental DNA in both lake cores.

detected by eDNA. In the Spring Lake eDNA record, *Castor* (beaver) appears between 5.4 and 3 cal. kyr BP, whereas evidence from Wood Bog[45] ~60 km to the south suggests that the beaver was part of the local fauna since at least 11 cal. kyr BP.

When the evidence from these multiple proxies is combined, it provides a more robust record of the presence of plants and animals than any single indicator. It is, of course, possible that some taxa arrived on the landscape earlier and escaped detection, thus appearing absent. However, there was only a narrow window of time between when the bottleneck region was beneath the waters of Glacial Lake Peace and

impassable, and when these proxies first detect the presence of plants and animals. The eDNA data are particularly important for indicating the earliest occurrence of terrestrial fauna in the bottleneck region, particularly the game animals that would have been key subsistence resources for hunter-gatherers[46].

Discussion

Although ice sheet retreat led to the corridor physically opening in the bottleneck region starting around 15–14 cal. kyr BP[10], deglaciation was followed by regional inundation below the waters of Glacial Lake Peace for perhaps up to 2,000 years[13]. By around 12.6 cal. kyr BP the ice sheets were several hundred kilometres apart and the landscape had become vegetated. Large and small animals came in soon thereafter, around 12.5 cal. kyr BP, making the corridor capable of supplying the biotic resources, including high-ranked prey such as bison, required by human foragers for the 1,500 km traverse[47]. This result is consistent with the recent finding that the oldest of the southern bison clade specimens (clades 1a and 2b) found north of the bottleneck region postdates 12.5 cal. kyr BP, though not with the finding that it opened earlier[3] (see Supplementary Information).

From our findings, it follows that an ice-free corridor was unavailable to those groups who appear to have arrived in the Americas south of the continental ice sheets by 14.7 cal. kyr BP[6,7], and also opened too late to have served as an entry route for the ancestors of Clovis who were present by 13.4 cal. kyr BP[1,9]. Not surprisingly, the earliest archaeological presence in the Peace River region, at Charlie Lake Cave (Fig. 3) and Saskatoon Mountain[45,47], postdates 12.6 cal. kyr BP. More striking, once opened, the corridor was not used just for southbound movement: archaeological evidence suggests that people were moving north as well, potentially renewing contact between groups that had been separated for millennia[1,9]. Bison[3] were also colonizing the corridor and moving north and south; it is uncertain whether other species, such elk[2] and brown bears[48], were moving similarly.

More broadly, although Clovis people may yet be shown to represent an independent migration separate from the peoples present here by 14,700 cal. kyr BP, they must have descended from a population that entered the Americas via a different route than the ice-free corridor. This conclusion is relevant to the recent finding[49] that ancestral Native Americans diverged into southern and northern branches ~13 cal. kyr BP (95% confidence interval of 14.5–11.5 cal. kyr BP). This implies that if that split occurred north of the ice sheets, there must have been two pulses of migration to the south. As the Anzick infant's genome, dated to 12.6 cal. kyr BP and associated with Clovis artefacts, is part of the southern branch[50], its ancestors must have travelled via the coast. However, this does not preclude the possibility that ancestors of the northern branch left Alaska later, through a then-viable ice-free corridor. Alternatively, if the divergence occurred in unglaciated North America, as recently proposed[49], it implies a single ancestral population came via the coast. It further raises the possibility that the
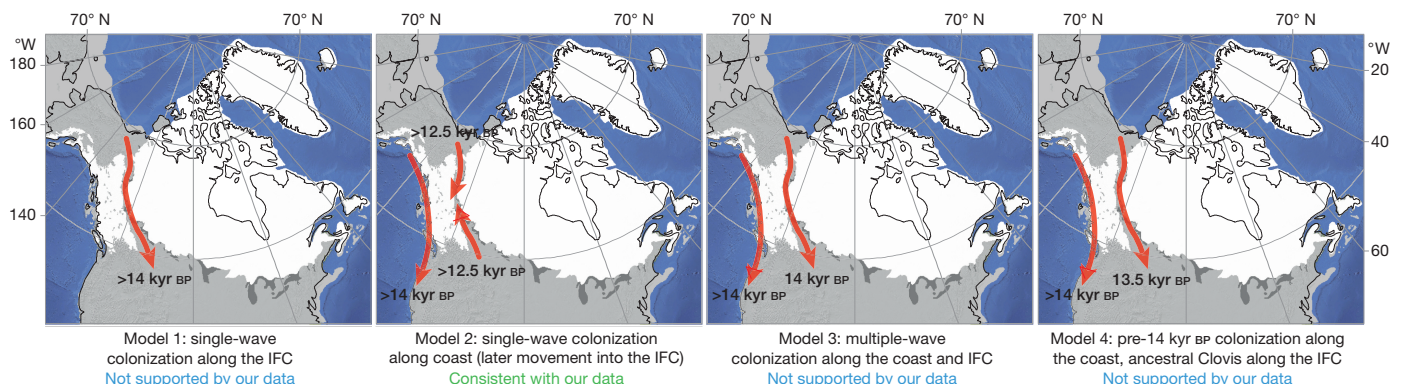

Figure 4 | Colonization models. Comparison of models of Paleoindian colonization (number of pulses, timing, and route(s)) that are supported or rejected by our data. All ages are in calibrated years before present.

northern branch—the descendants occupying Alaska today—made their way north to Alaska via the corridor after 12.6 cal. kyr BP. Further investigations of ancient DNA may help resolve this issue.

1. Ives, J. W., Froese, D., Supernant, K. & Yanicki, G. M. *Paleoamerican Odyssey* 149–169 (Texas A & M Univ. Press, 2014).
2. Meiri, M. *et al.* Faunal record identifies Bering isthmus conditions as constraint to end-Pleistocene migration to the New World. *Proc. R. Soc. Lond. B* **281,** 20132167 (2013).
3. Heintzman, P. D. *et al.* Bison phylogeography constrains dispersal and viability of the Ice Free Corridor in western Canada. *Proc. Natl Acad. Sci. USA* **113,** 8057–8063 (2016).
4. Ferring, C. R. *The Archaeology and Paleoecology of the Aubrey Clovis Site (41DN479)* (Denton County, 2001).
5. Sanchez, G. *et al.* Human (Clovis)-gomphothere (*Cuvieronius* sp.) association ∼ 13,390 calibrated yBP in Sonora, Mexico. *Proc. Natl Acad. Sci. USA* **111,** 10972–10977 (2014).
6. Dillehay, T. D. *et al.* Monte Verde: seaweed, food, medicine, and the peopling of South America. *Science* **320,** 784–786 (2008).
7. Gilbert, M. T. P. *et al.* DNA from pre-Clovis human coprolites in Oregon, North America. *Science* **320,** 786–789 (2008).
8. Dillehay, T. D. *et al.* New archaeological evidence for an early human presence at Monte Verde, Chile. *PLoS One* **10,** e0141923 (2015).
9. Meltzer, D. J. *First Peoples in a New World: Colonizing Ice Age America* (Univ. California Press, 2009).
10. Dyke, A. S. An outline of North American deglaciation with emphasis on central and northern Canada. *Quaternary Glaciations: Extent and Chronology* 371–406 (Elsevier, 2004).
11. Dixon, E. J. Late Pleistocene colonization of North America from northeast Asia: new insights from large-scale paleogeographic reconstructions. *Quat. Int.* **285,** 57–67 (2013).
12. Madsen, D. B. A framework for the initial occupation of the Americas. *PaleoAmerica* **1,** 217–250 (2015).
13. Hickin, A. S., Lian, O. B., Levson, V. M. & Cui, Y. Pattern and chronology of glacial Lake Peace shorelines and implications for isostasy and ice-sheet configuration in northeastern British Columbia, Canada. *Boreas* **44,** 288–304 (2015).
14. Hickin, A. S., Lian, O. B. & Levson, V. M. Coalescence of late Wisconsinan Cordilleran and Laurentide ice sheets east of the Rocky Mountain foothills in the Dawson Creek region, northeast British Columbia, Canada. *Quat. Res.* **85,** 409–429 (2016).
15. Munyikwa, K., Feathers, J. K., Rittenour, T. M. & Shrimpton, H. K. Constraining the Late Wisconsinan retreat of the Laurentide ice sheet from western Canada using luminescence ages from postglacial aeolian dunes. *Quat. Geochronol.* **6,** 407–422 (2011).
16. White, J. M., Mathewes, R. W. & Mathews, W. H. Late Pleistocene chronology and environment of the 'ice-free corridor' of northwestern Alberta. *Quat. Res.* **24,** 173–186 (1985).
17. James Dixon, E. Human colonization of the Americas: timing, technology and process. *Quat. Sci. Rev.* **20,** 277–299 (2001).
18. Viereck, L. A. Plant succession and soil development on gravel outwash of the Muldrow Glacier, Alaska. *Ecol. Monogr.* **36,** 181–199 (1966).
19. Mandryk, C. A. S., Josenhans, H., Fedje, D. W. & Mathewes, R. W. Late Quaternary paleoenvironments of northwestern North America: implications for inland versus coastal migration routes. *Quat. Sci. Rev.* **20,** 301–314 (2001).
20. Stokes, C. R., Margold, M., Clark, C. D. & Tarasov, L. Ice stream activity scaled to ice sheet volume during Laurentide Ice Sheet deglaciation. *Nature* **530,** 322–326 (2016).
21. Gowan, E. J. An assessment of the minimum timing of ice free conditions of the western Laurentide Ice Sheet. *Quat. Sci. Rev.* **75,** 100–113 (2013).
22. Mathews, W. H. Quaternary stratigraphy and geomorphology of Charlie Lake (94a) map area, British Columbia. *Canadian Geological Survey* http://dx.doi.org/10.4095/104544 (1978).
23. White, J. M., Mathewes, R. W. & Mathews, W. H. Radiocarbon dates from Boone Lake and their relation to the 'ice-free corridor' in the Peace River district of Alberta, Canada. *Can. J. Earth Sci.* **16,** 1870–1874 (1979).
24. Hartman, G. & Clague, J. J. Quaternary stratigraphy and glacial history of the Peace River valley, northeast British Columbia. *Can. J. Earth Sci.* **45,** 549–564 (2008).
25. Birks, H. H. & Birks, H. J. B. *Quaternary Palaeoecology* (Edward Arnold, 1980).
26. Jass, C. N., Burns, J. A. & Milot, P. J. Description of fossil muskoxen and relative abundance of Pleistocene megafauna in central Alberta. *Can. J. Earth Sci.* **48,** 793–800 (2011).
27. Kooyman, B., Hills, L. V., McNeil, P. & Tolman, S. Late Pleistocene horse hunting at the Wally's Beach site (DhPg-8), Canada. *Am. Antiq.* **71,** 101–121 (2006).
28. Burns, J. A. Mammalian faunal dynamics in Late Pleistocene Alberta, Canada. *Quat. Int.* **217,** 37–42 (2010).
29. Kooyman, B., Hills, L., Tolman, S. & McNeil, P. Late Pleistocene western camel (*Camelops hesternus*) hunting in southwestern Canada. *Am. Antiquity* **77,** 115–124 (2012).
30. Faegri, K., Kaland, P. E. & Krzywinski, K. *Textbook of Pollen Analysis* 1–328 (John Wiley and Sons, 1990).
31. Bennett, K. D. *Documentation for PSIMPOLL 4.10 and PSCOMB 1.03.* 1–127 (Univ. of Uppsala, Sweden, 2005).
32. Willerslev, E. *et al.* Diverse plant and animal genetic records from Holocene and Pleistocene sediments. *Science* **300,** 791–795 (2003).
33. Pedersen, M. W. *et al.* Ancient and modern environmental DNA. *Proc. R. Soc. Lond. B* http://dx.doi.org/10.1098/rstb.2013.0383 (2015).
34. Pedersen, M. W. *et al.* A comparative study of ancient environmental DNA to pollen and macrofossils from lake sediments reveals taxonomic overlap and additional plant taxa. *Quat. Sci. Rev.* **75,** 161–168 (2013).
35. Parducci, L. *et al.* Molecular- and pollen-based vegetation analysis in lake sediments from central Scandinavia. *Mol. Ecol.* **22,** 3511–3524 (2013).
36. Haile, J. *et al.* Ancient DNA reveals late survival of mammoth and horse in interior Alaska. *Proc. Natl Acad. Sci. USA* **106,** 22352–22357 (2009).
37. Parducci, L. *et al.* Glacial survival of boreal trees in northern Scandinavia. *Science* **335,** 1083–1086 (2012).
38. Valentini, A., Pompanon, F. & Taberlet, P. DNA barcoding for ecologists. *Trends Ecol. Evol.* **24,** 110–117 (2009).
39. Coissac, E., Hollingsworth, P. M., Lavergne, S. & Taberlet, P. From barcodes to genomes: extending the concept of DNA barcoding. *Mol. Ecol.* **25,** 1423–1428 (2016).
40. Jónsson, H., Ginolhac, A., Schubert, M., Johnson, P. L. F. & Orlando, L. mapDamage2.0: fast approximate Bayesian estimates of ancient DNA damage parameters. *Bioinformatics* **29,** 1682–1684 (2013).
41. Hickman, M. & White, J. Late Quaternary palaeoenvironment of Spring Lake, Alberta, Canada. *J. Paleolimnol.* **2,** 305–317 (1989).
42. Godwin, H. Pollen analysis, an outline of the problems and potentialities of the method. Part I. Technique and interpretation. *New Phytol.* **33,** 278–305 (1934).
43. Hebda, R. J., Burns, J. A., Geertsema, M. & Timothy Jull, A. J. AMS-dated late Pleistocene taiga vole (Rodentia: *Microtus xanthognathus*) from northeast British Columbia, Canada: a cautionary lesson in chronology. *Can. J. Earth Sci.* **45,** 611–618 (2008).
44. Harington, C. R. Quaternary cave faunas of Canada: a review of the vertebrate remains. *J. Caves Karst Stud.* **73,** 162–180 (2009).
45. Beaudoin, A. B., Wright, M. & Ronaghan, B. Late quaternary landscape history and archaeology in the 'Ice-Free Corridor': Some recent results from Alberta. *Quat. Int.* **32,** 113–126 (1996).
46. Potter, B. A., Holmes, C. & Yesner, D. R. *Paleoamerican Odyssey* 81–103 (Texas A & M Univ. Press, 2014).
47. Driver, J. C. & Vallières, C. The Palaeoindian bison assemblage from Charlie Lake Cave, British Columbia. *Can. J. Archaeol.* **32,** 239–257 (2008).
48. Matheus, P., Burns, J., Weinstock, J. & Hofreiter, M. Pleistocene brown bears in the mid-continent of North America. *Science* **306,** 1150 (2004).
49. Raghavan, M. *et al.* Genomic evidence for the Pleistocene and recent population history of Native Americans. *Science* **349,** http://dx.doi.org/10.1126/science.aab3884 (2015).
50. Rasmussen, M. *et al.* The genome of a Late Pleistocene human from a Clovis burial site in western Montana. *Nature* **506,** 225–229 (2014).

Author Contributions E.W. initiated and led the study. M.W.P., K.H.K., and E.W. designed and conducted the study. A.R., C.S., C.Z. and H.F. processed and counted pollen and macrofossils. R.A.S. performed the ¹⁴C dating and Bayesian age modelling. N.K.L. and R.A.R. scanned cores for X-ray fluorescence and magnetic susceptibility. K.K.K., M.W.P. and K.H.K. performed the cartographic analysis and representation. M.L.Z.M. and M.W.P. processed and analysed the metabarcode data set. M.W.P. performed the molecular work under supervision by L.O. and E.W. M.W.P., C.S., A.B.B., B.A.P., D.J.M., K.H.K. and E.W. did the main interpretations of the results, with additional statistical analysis from R.N. M.W.P., D.J.M. and E.W. wrote the paper with input from all authors.

Author Information DNA sequence data are available through the European Nucleotide Archive under accession number PRJEB14494 and bioinformatics scripts are available at (https://github.com/ancient-eDNA/Holi). Reprints and permissions information is available at www.nature.com/reprints. The authors declare no competing financial interests. Readers are welcome to comment on the online version of the paper. Correspondence and requests for materials should be addressed to E.W. (ewillerslev@snm.ku.dk).

Reviewer Information *Nature* thanks P. Gibbard, S. McGowan, A. P. Roberts and the other anonymous reviewer(s) for their contribution to the peer review of this work.

METHODS

Data reporting. No statistical methods were used to predetermine sample size. The experiments were not randomized. The investigators were not blinded to allocation during experiments and outcome assessment.

Sediment sampling. We obtained 23 sediment cores from 8 different lakes by using a percussion corer deployed from the frozen lake surface[51]. To prevent eventual internal mixing, we discarded all upper suspended sediments and only kept the compacted sediment for further investigation. Cores were cut into smaller sections to allow transport and storage. All cores were taken to laboratories at the University of Calgary and were stored cold at 5 °C until subsequent subsampling. Cores were split using an adjustable tile saw, cutting only the PVC pipe. The split half was taken into a positive pressure laboratory for DNA subsampling. DNA samples were taken wearing full body suit, mask and sterile gloves; the top 10 mm were removed using two sterile scalpels and samples were taken with a 5 ml sterile disposable syringe (3–4 cm^2) and transferred to a 15 ml sterile spin tube. Caution was taken not to cross-contaminate between layers or to sample sediments in contact with the inner side of the PVC pipe. Samples were taken every centimetre in the lowest 1 m of the core (except for Spring Lake, the lowest 2 m), then intervals of 2 cm higher up, and finally samples were taken every 5 cm, and subsequently frozen until analysed. Pollen samples were taken immediately next to the DNA samples, while macrofossil samples were cut from the remaining layer in 1 cm or 2 cm slices. Following sampling, the second intact core halves were visually described and wrapped for transport. All cores were stored at 5 °C before, during and after shipment to the University of Copenhagen (Denmark).

Core logging and scanning. An ITRAX core scanner was used to take high-resolution images and to measure magnetic susceptibility at the Department of Geoscience, Aarhus University. Magnetic susceptibility[52] was measured every 0.5 cm using a Bartington Instruments MS2 system (Extended Data Fig. 2).

Pollen and macrofossil extraction and identification. Pollen was extracted using a standard protocol[30]. *Lycopodium* markers were added to determine pollen concentrations[53] (see Supplementary Information). Samples were mounted in (2000 cs) silicone oil and pollen including spores were counted using a Leica Laborlux-S microscope at 400× magnification and identified using keys[30,53,54] as well as reference collections of North American and Arctic pollen housed at the University of Alberta and the Danish Natural History Museum, respectively. Pollen and pteridophyte spores were identified at least to family level and, more typically, to genera. Green algae coenobia of *Pediastrum boryanum* and *Botryococcus* were recorded to track changes in lake trophic status. Pollen influx values were calculated using pollen concentrations divided by the deposition rate (see Supplementary Information). Microfossil diagrams were produced and analysed using PSIMPOLL 4.10 (ref. 31). The sequences were zoned with CONIIC[31], with a stratigraphy constrained clustering technique using the information statistic as a distance measure. All macrofossils were retrieved using a 100 μm mesh size and were identified but not quantified.

Radiocarbon dating and age-depth modelling. Plant macrofossils identified as terrestrial taxa (or unidentifiable macrofossils with terrestrial characteristics where no preferable material could be identified) were selected for radiocarbon (^{14}C) dating of the lacustrine sediment. All macrofossils were subjected to a standard acid-base-acid (ABA) chemical pre-treatment at the Oxford Radiocarbon Accelerator Unit (ORAU), following a standard protocol[55], with appropriate 'known age' (that is, independently dendrochronologically-dated tree-ring) standards run alongside the unknown age plant macrofossil samples[56]. Specifically, this ABA chemical pre-treatment (ORAU laboratory pre-treatment code 'VV') involved successive 1 M HCl (20 min, 80 °C), 0.2 M NaOH (20 min, 80 °C) and 1 M HCl (1 h, 80 °C) washes, with each stage followed by rinsing to neutrality (≥3 times) with ultrapure MilliQ deionised water. The three principal stages of this process (successive ABA washes) are similar across most radiocarbon laboratories and are, respectively, intended to remove: (i) sedimentary- and other carbonate contaminants; (ii) organic (principally humic- and fulvic-) acid contaminants; and (iii) any dissolved atmospheric CO_2 that might have been absorbed during the preceding base wash. Thus, any potential secondary carbon contamination was removed, leaving the samples pure for combustion and graphitisation. Accelerator mass spectrometry (AMS) ^{14}C dating was subsequently performed on the 2.5 MV HVEE tandem AMS system at ORAU[57]. As is standard practice, measurements were corrected for natural isotopic fractionation by normalizing the data to a standard δ^{13}C value of −25‰ VPDB, before reporting as conventional ^{14}C ages before present (BP, before AD 1950)[58].

These ^{14}C data were calibrated with the IntCal13 calibration curve[59] and modelled using the Bayesian statistical software OxCal v. 4.2 (ref. 60). Poisson process ('P_Sequence') deposition models were applied to each of the Charlie and

Spring Lake sediment profiles[61], with objective 'Outlier' analysis applied to each of the constituent ^{14}C determinations[62]. The P_Sequence model takes into account the complexity (randomness) of the underlying sedimentation process, and thus provides realistic age-depth models for the sediment profiles on the calibrated radiocarbon (IntCal) timescale. The rigidity of the P_Sequence (the regularity of the sedimentation rate) is determined iteratively within OxCal through a model averaging approach, based upon the likelihood (calibrated ^{14}C) data included within the model[60]. A prior 'Outlier' probability of 5% was applied to each of the ^{14}C determinations, because there was no reason, a priori, to believe that any samples were more likely to be statistical outliers than others. All ^{14}C determinations are provided in Extended Data Table 1; OxCal model coding is provided in the Supplementary Information; and plots of the age-depth models derived for Spring and Charlie Lakes are given in Extended Data Fig. 2.

DNA analysis. All DNA extractions and pre-PCR analyses were performed in the ancient DNA facilities of the Centre for GeoGenetics, Copenhagen. Total genomic DNA was extracted using a modified version of an organic extraction protocol[63]. We used a lysis buffer containing 68 mM *N*-lauroylsarcosine sodium salt, 50 mM Tris-HCl (pH 8.0), 150 mM NaCl, and 20 mM EDTA (pH 8.0) and, immediately before extraction, 1.5 ml 2-mercaptoethanol and 1.0 ml 1 M DTT were added for each 30 ml lysis buffer. Approximately 2 g of sediment was added, and 3 ml of buffer, together with 170 μg of proteinase K, and vortexed vigorously for 2× 20 s using a FastPrep-24 at speed 4.0 m s^{-1}. An additional 170 μg of proteinase K was added to each sample and incubated, gently rotating overnight at 37 °C. For removal of inhibitors we used the MOBIO (MO BIO Laboratories, Carlsbad, CA) C2 and C3 buffers following the manufacturer's protocol. The extracts were further purified using phenol-chloroform and concentrated using 30 kDa Amicon Ultra-4 centrifugal filters as described in the Andersen extraction protocol[63]. Our extraction method was changed from this protocol with the following modifications: no lysis matrix was added due to the minerogenic nature of the samples and the two phenol, one chloroform step was altered, thus both phenol:chloroform:supernatant were added simultaneously in the respective ratio 1:0.5:1, followed by gentle rotation at room temperature for 10 min and spun for 5 min at 3,200*g*. For dark-coloured extracts, this phenol:chloroform step was repeated. All extracts were quantified using Quant-iT dsDNA HS assay kit (Invitrogen) on a Qubit 2.0 Fluorometer according to the manufacturer's manual. The measured concentrations were used to calculate the total ng DNA extracted per g of sediment (Fig. 2). 32 samples were prepared for shotgun metagenome sequencing[64] using the NEBNext DNA Library Prep Master Mix Set for 454 (New England BioLabs) following the manufacturer's protocol with the following modifications: (i) all reaction volumes (except for the end repair step) were decreased to half the size as in the protocol, and (ii) all purification steps were performed using the MinElute PCR Purification kit (Qiagen). Metagenome libraries were amplified using AmpliTaq Gold (Applied Biosystems), given 14–20 cycles following and quantified using the 2100 BioAnalyser chip (Agilent). All libraries were purified using Agencourt AMPure XP beads (BeckmanCoulter), quantified on the 2100 BioAnalyzer and pooled equimolarly. All pooled libraries were sequenced on an Illumina HiSeq 2500 platform and treated as single-end reads.

Bioinformatics. Metagenomic reads were demultiplexed and trimmed using AdapterRemoval 1.5 (ref. 65) with a minimum base quality of 30 and minimum length of 30 bp[66]. All reads with poly-A/T tails ≥ 4 were removed from each sample. Low-quality reads and duplicates were removed using String Graph Assembler (SGA)[67] setting the preprocessing tool dust-threshold = 1, index algorithm = 'ropebwt' and using the SGA filter tool to remove exact and contained duplicates. Each quality-controlled (QC) read was thereafter allowed equal change to map to reference sequences using Bowtie2 version 2.2.4 (ref. 68) (end-to-end alignment and mode –k 50 for example, reads were allowed a total of 500 hits before being parsed). A few reads with more than 500 matches were confirmed by checking that the best blast hit belonged to this taxon, and that alternative hits have lower e-values and alignment scores. We used the full nucleotide database (nt) from GenBank (accessed 4 March 2015), which due to size and downstream handling was divided into 9 consecutive equally sized databases and indexed using Bowtie2-build. All QC checked fastq files were aligned end-to-end using Bowtie2 default settings. Each alignment was merged using SAMtools[69], sorted according to read identifier and imported to MEGAN v. 10.5 (ref. 70). We performed a lowest common ancestor (LCA) analysis using the built-in algorithm in MEGAN and computed the taxonomic assignments employing the embedded NCBI taxonomic tree (March 2015 version) on reads having 100% matches to a reference sequence. We call this pipeline 'Holi' because it takes a holistic approach because it has no a priori assumption of environment and the read is given an equal chance to align against the nt database containing the vast majority of organismal

sequences (see Supplementary Information). *In silico* testing of 'Holi' sensitivity (see Supplementary Information) revealed 0.1% as a reliable minimum threshold for Viridiplantae taxa. For metazoan reads, which were found to be under-represented in our data, we set this threshold to 3 unique reads in one sample or 3 unique reads in three different samples from the same lake. In addition, we confirmed that each read within the metazoans by checking that the best blast hit belonged to this taxon, and that alternative hits have lower *e*-values and alignment scores[71]. We merged all sequences from all blanks and subtracted this from the total data set (instead of pairing for each extract and library build), using lowest taxonomic end nodes. Candidate detection was performed by decreasing the detection threshold in 'Holi' from 0.1% to 0.01% to increase the detection of contaminating plants, and similar for metazoans, we decreased the detection level and subtracted all with 2 or more reads per taxa (see Supplementary Information). We performed a series of *in silico* tests to measure the sensitivity and specificity of our assignment method and to estimate likelihood of false-positives (see Supplementary Information).

We generated 1,030,354,587 Illumina reads distributed across 32 sediment samples and used the dedicated computational pipeline ('Holi') for handling read de-multiplexing, adaptor trimming, control quality, duplicate and low-complexity read removal (see Supplementary Information). The 257,890,573 reads parsing filters were further aligned against the whole non-redundant nucleotide (nt) sequence database[72]. Hereafter, we used a lowest common ancestor approach[70] to recover taxonomic information from the 985,818 aligning reads. Plants represented by less than 0.1% of the total reads assigned were discarded to limit false positives resulting from database mis-annotations, PCR and sequencing errors (see Supplementary Information). Given the low number of reads assigned to multicellular, eukaryotic organisms (metazoans), we set a minimal threshold of 3 counts per sample or 1 count in each of three samples. For plants and metazoans this resulted in 511,504 and 2,596 reads assigned at the family or genus levels, respectively. The read counts were then normalized for generating plant and metazoan taxonomic profiles (Extended Data Figs 5 and 6). Taxonomic profiles for reads assigned to bacteria, archaea, fungi and alveolata were also produced (see Supplementary Information).

DNA damage and authenticity. We estimated the DNA damage levels using the MapDamage package 2.0 (ref. 40) for the most abundant organisms (Extended Data Fig. 7b). These represent distinctive sources, which help to account for potential differences between damage accumulated from source to deposition or during deposition. Input SAM files were generated for each sample using Bowtie2 (ref. 68) to align all QC reads from each sample against each reference genome. All aligning sequences were converted to BAM format, sorted and parsed through MapDamage by running the statistical estimation using only the 5′-ends (–forward) for single reads. All frequencies of cytosine to thymine mutations per position from the 5′ ends were parsed and the standard deviation was calculated to generate DNA damage models for each lake (Extended Data Fig. 7a and Supplementary Information).

51. Reasoner, M. A. Equipment and procedure improvements for a lightweight, inexpensive, percussion core sampling system. *J. Paleolimnol.* **8,** 273–281 (1993).
52. Sandgren, P. & Snowball, I. *Tracking Environmental Change Using Lake Sediments: Physical and Geochemical Methods* Vol. 2, 217–236 (Kluwer Academic Publishers, 2001).
53. Moore, P. D., Webb, J. A. & Collison, M. E. *Pollen Analysis* 1–216 (Blackwell Scientific Publications, 1991).
54. Beug, H. J. *Leitfaden der Pollenbestimmung* 74–90 (Verlag Dr. Friedrich Pfeil, 2004).
55. Brock, F., Higham, T., Ditchfield, P. & Bronk Ramsey, C. Current pretreatment methods for AMS radiocarbon dating at the Oxford Radiocarbon Accelerator Unit (ORAU). *Radiocarbon* **52,** 103–112 (2010).
56. Staff, R. Wood pretreatment protocols and measurement of tree-ring standards at the Oxford Radiocarbon Accelerator Unit (ORAU). *Radiocarbon* **56,** 709–715 (2014).
57. Bronk Ramsey, C., Higham, T. & Leach, P. Towards high-precision AMS: progress and limitations. *Radiocarbon* **46,** 17–24 (2004).
58. Stuiver, M. & Polach, H. Reporting of ^{14}C data. *Radiocarbon* **19,** 355–364 (1977).
59. Reimer, P. J., Bard, E., Bayliss, A. & Beck, J. W. IntCal13 and Marine13 radiocarbon age calibration curves 0–50,000 years cal. BP. *Radiocarbon* **55,** 1869–1887 (2013).
60. Bronk Ramsey, C. & Lee, S. Recent and planned developments of the program OxCal. *Radiocarbon* **55,** 720–730 (2013).
61. Bronk Ramsey, C. Deposition models for chronological records. *Quat. Sci. Rev.* **27,** 42–60 (2008).
62. Bronk Ramsey, C. Dealing with outliers and offsets in radiocarbon dating. *Radiocarbon* **51,** 1023–1045 (2009).
63. Wales, N., Andersen, K., Cappellini, E., Avila-Arcos, M. C. & Gilbert, M. T. Optimization of DNA recovery and amplification from non-carbonized archaeobotanical remains. *PLoS One* **9,** e86827 (2014).
64. Meyer, M. & Kircher, M. Illumina sequencing library preparation for highly multiplexed target capture and sequencing. *Cold Spring Harb. Protoc.* **2010,** http://dx.doi.org/10.1101/pdb.prot5448 (2010).
65. Lindgreen, S. AdapterRemoval: easy cleaning of next-generation sequencing reads. *BMC Res. Notes* **5,** 337 (2012).
66. Schubert, M. *et al.* Improving ancient DNA read mapping against modern reference genomes. *BMC Genomics* **13,** 178 (2012).
67. Simpson, J. T. & Durbin, R. Efficient de novo assembly of large genomes using compressed data structures. *Genome Res.* **22,** 549–556 (2012).
68. Langmead, B. & Salzberg, S. L. Fast gapped-read alignment with Bowtie 2. *Nat. Methods* **9,** 357–359 (2012).
69. Li, H. *et al.* The sequence alignment/map format and SAMtools. *Bioinformatics* **25,** 2078–2079 (2009).
70. Huson, D. H., Auch, A. F., Qi, J. & Schuster, S. C. MEGAN analysis of metagenomic data. *Genome Res.* **17,** 377–386 (2007).
71. Altschul, S. F., Gish, W., Miller, W., Myers, E. W. & Lipman, D. J. Basic local alignment search tool. *J. Mol. Biol.* **215,** 403–410 (1990).
72. NCBI. Nt Database. (ftp:// ftp. ncbi. nih. gov/ blast/ db/ FASTA/ nt. gz) (February 2015).
73. Bronk Ramsey, C. Bayesian analysis of radiocarbon dates. *Radiocarbon* **51,** 337–360 (2009).
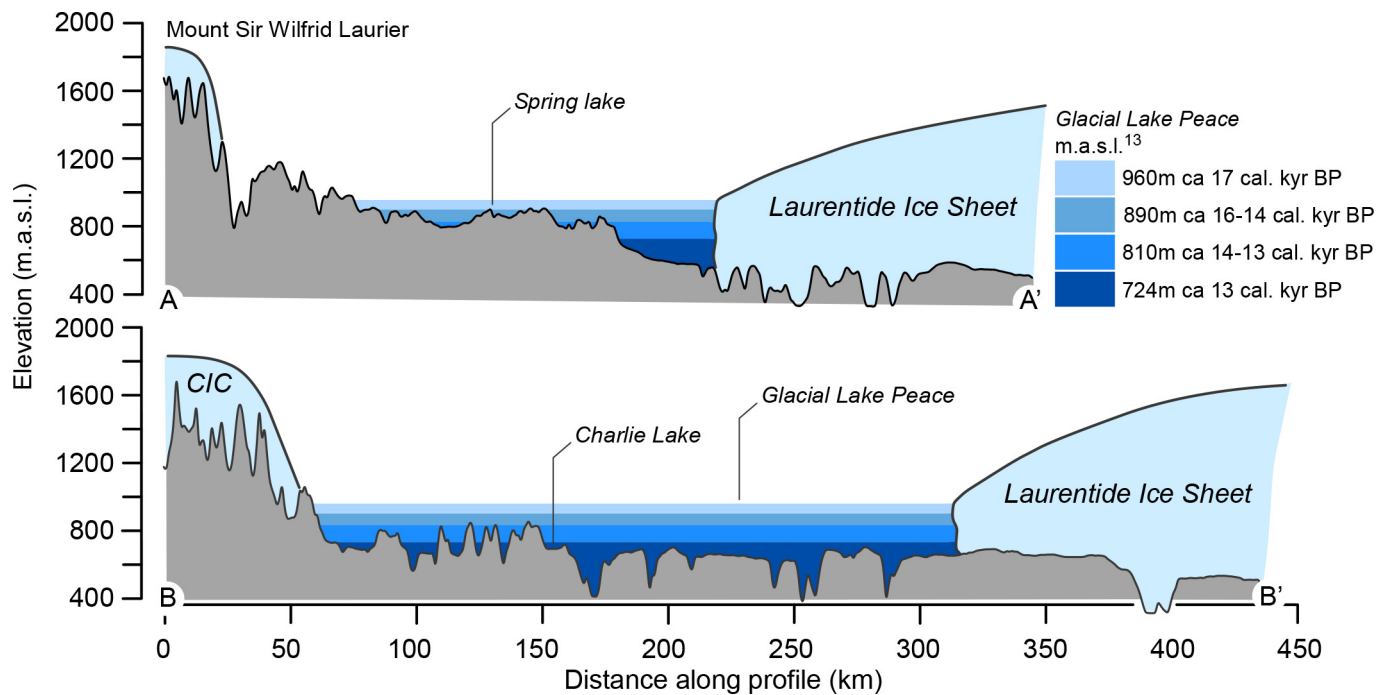
Extended Data Figure 1 | Topographic transects. The red and white lines on Fig. 1b mark topographic transects of Charlie Lake and Spring Lake in relation to the four phases of Glacial Lake Peace[13]. CIC, Cordilleran ice complex; m.a.s.l., metres above sea level.
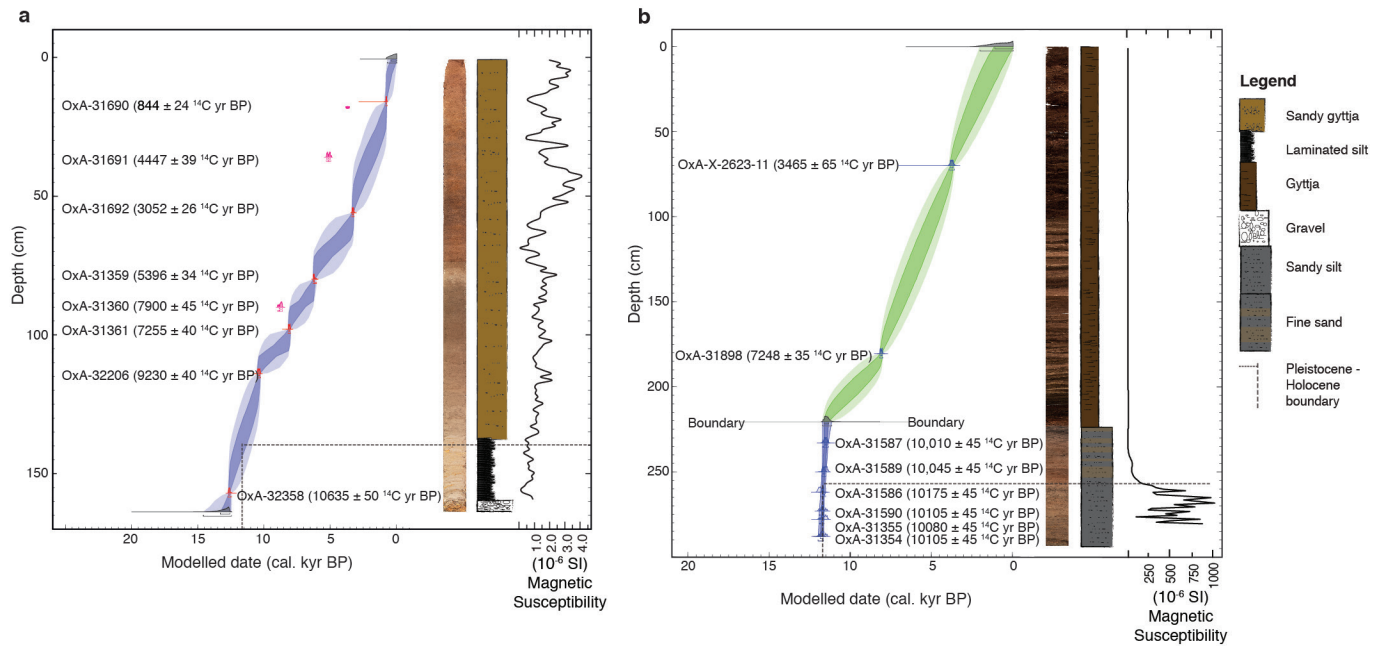
Extended Data Figure 2 | Visual and physical descriptions and age-depth model for the studied lake sediments. a, **b**, Charlie Lake (**a**) and Spring Lake (**b**) span the Pleistocene to Holocene transition (dotted grey line); magnetic susceptibility (continuous black line); and compressed high-resolution images from the ITRAX core scanner and the sedimentary log are shown. Age-depth models for Charlie Lake (**a**) and Spring Lake (**b**) were generated with P_Sequence deposition models in OxCal v. 4.2 using the IntCal13 radiocarbon calibration curve[57,59,61]. The probability envelopes represent the 68.2% and 95.4% confidence ranges, respectively (see Methods and Supplementary Information).
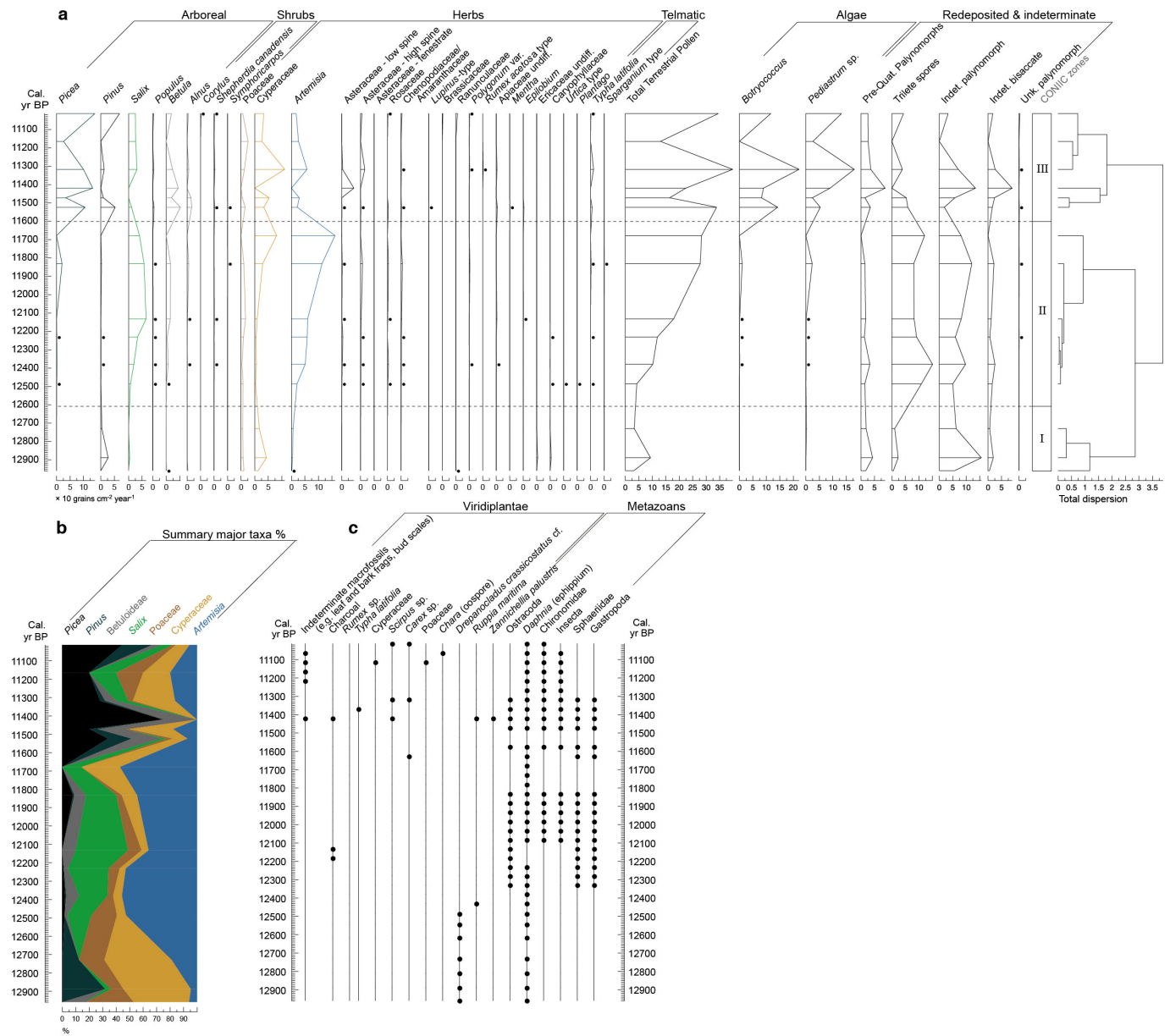
Extended Data Figure 3 | Charlie Lake pollen and macrofossil diagrams. a, Pollen are presented as influx and bullet points indicate taxa with less than 2 grains cm^{-2} year^{-1}. The diagram was zoned using CONIIC[31] with a stratigraphically constrained cluster analysis on the information statistic. **b**, Relative proportions of ecologically important taxa. **c**, Macrofossils were identified but not enumerated. Bullet points represent presence.

Extended Data Figure 4 | Spring Lake pollen and macrofossil diagrams. a, Pollen are presented as influx and bullet points represent taxa with less than 50 grains cm^{-2} year^{-1}. The diagram was zoned using CONIIC[31] with a stratigraphically constrained cluster analysis on the information statistic. **b**, Relative proportions of ecologically important taxa. **c**, Macrofossils were identified but not enumerated. Bullet points represent presence.
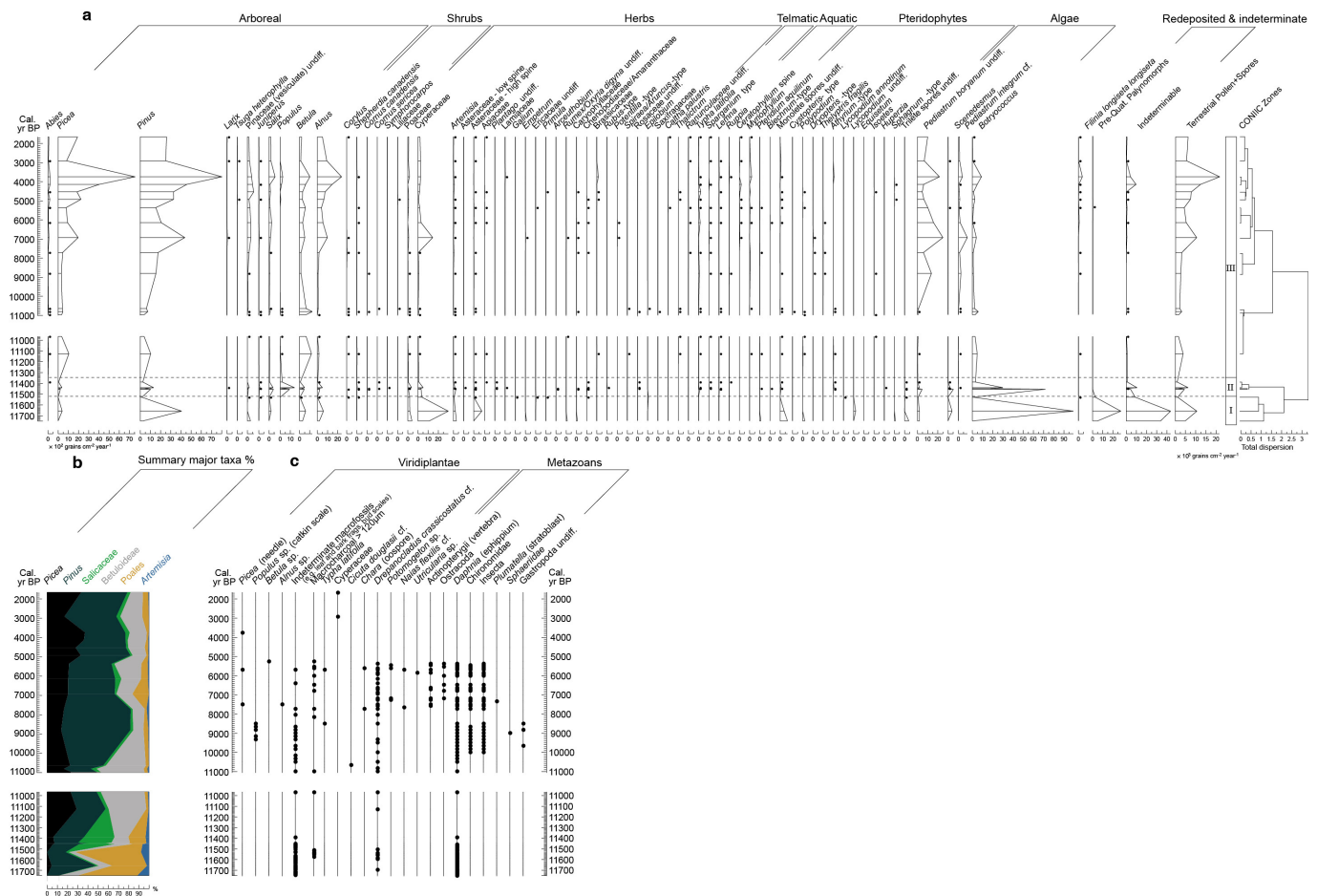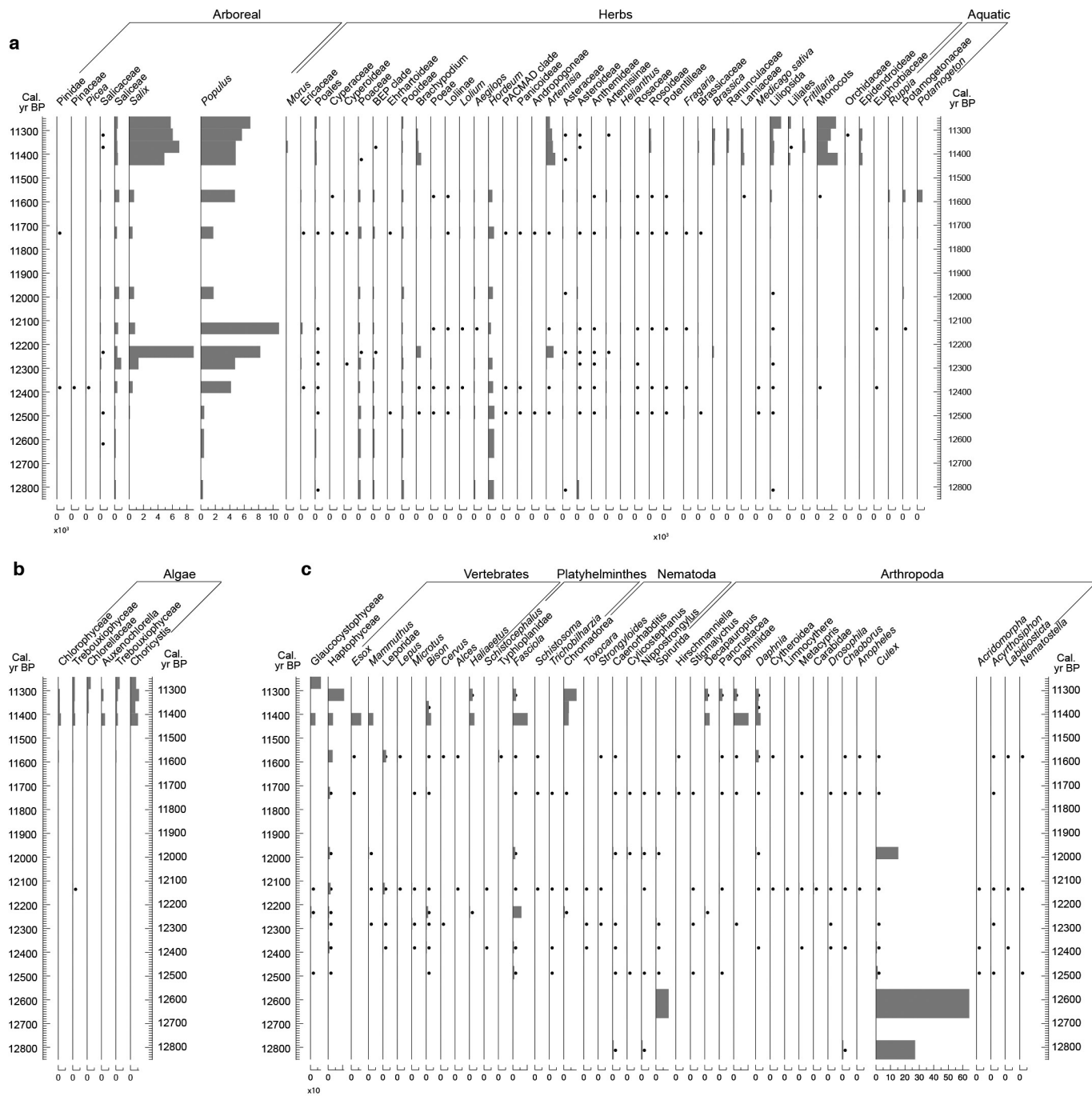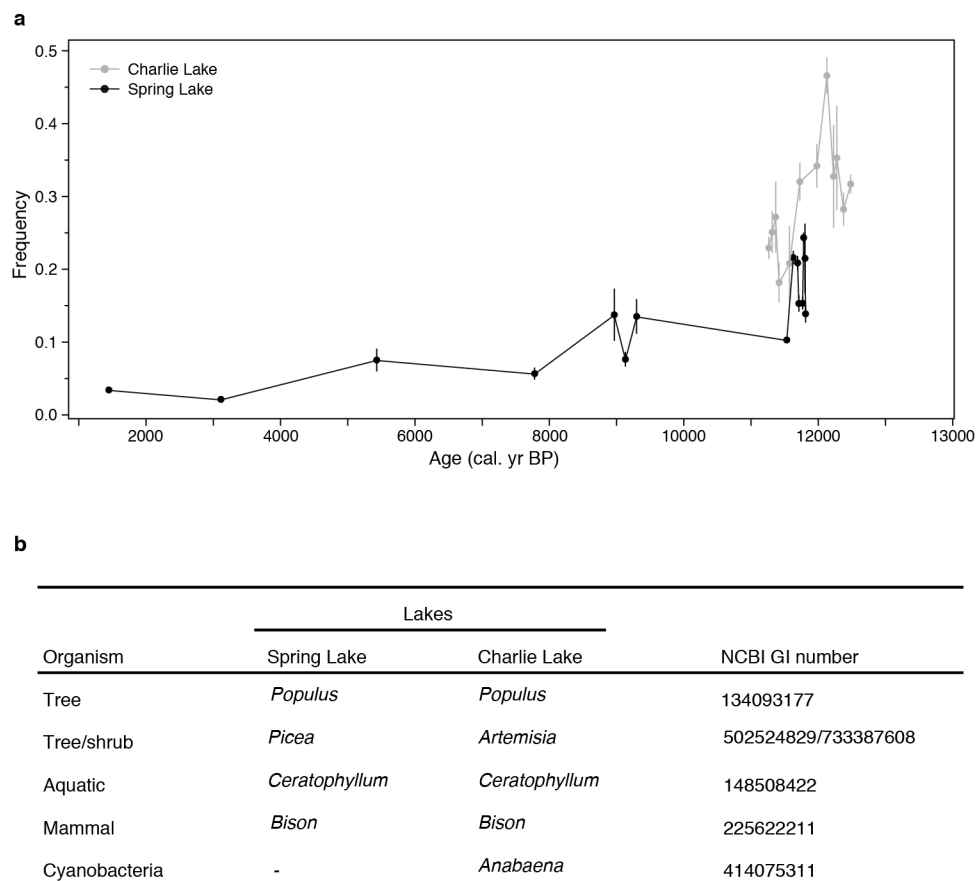
Extended Data Figure 5 | Charlie Lake DNA diagram. DNA results are presented as normalized counts to allow comparison on the temporal scale for each taxon. All are unique sequences with 100% sequence identity to taxa. Histogram width equals the accumulation period. **a**, Viridiplantae, bullet points represent counts less than 50. **b**, Algae, bullet points represent counts less than 50. **c**, Metazoans, bullet points represent counts equal to 1.

Extended Data Figure 6 | Spring Lake DNA diagram. DNA results are presented as normalized counts to allow comparison on the temporal scale for each taxon. All are unique sequences with 100% sequence identity to taxa. Histogram width equals the accumulation period. **a**, Viridiplantae, bullet points represent counts less than 50. **b**, Algae, bullet points represent counts less than 50. **c**, Metazoans, bullet points represent counts equal to 1.

a

b

	Lakes		
Organism	Spring Lake	Charlie Lake	NCBI GI number
Tree	*Populus*	*Populus*	134093177
Tree/shrub	*Picea*	*Artemisia*	502524829/733387608
Aquatic	*Ceratophyllum*	*Ceratophyllum*	148508422
Mammal	*Bison*	*Bison*	225622211
Cyanobacteria	-	*Anabaena*	414075311

Extended Data Figure 7 | DNA damage accumulation model. Maximum-likelihood DNA damage rates were estimated from nucleotide misincorporation patterns using MapDamage2.0 (ref. 40). **a**, Each full circle is the mean of cytosine to thymine mutation frequencies at the first position ($n \geq 2$ species) with above 500 reads aligned to reference bars that represent ± 1 s.d. **b**, Table of species used for determining the DNA damage rates.

Extended Data Table 1 | AMS ^{14}C determinations of terrestrial plant macrofossil samples from Charlie and Spring Lakes

Sample ID	AMS Laboratory code	Depth (cm)	Conventional ^{14}C Age (yrs BP ± 1s) unless stated (ref. 82)	d^{13}C (‰)	Modeled, calibrated age (cal. BP)		Posterior / Prior Outlier probability (%)	Material dated
					68.2% probability range	95.4% probability range		
Charlie Lake								
MWP_30	OxA-31690	16	844 ± 24	-24.9	782 - 730	797 - 690	5 / 5	Unid. terrestrial and charred plants
MWP_31	OxA-31691 *	36	4447 ± 39	-26.0	*	*	(81 /5) *	Unidentifiable terrestrial plants
MWP_32	OxA-31692	56	3052 ± 26	-27.9	3335 - 3216	3353 - 3180	3 / 5	Unidentifiable terrestrial plants
MWP_20	OxA-31359	80	5396 ± 34	-21.3	6276 - 6188	6289 - 6024	3 / 5	Unidentifiable terrestrial plants
MWP_21	OxA-31360 *	90	7900 ± 45	-24.0	*	*	(70 / 5) *	*Cyperus* sp. + *Carex* sp. (seed)
MWP_22	OxA-31361	98	7255 ± 40	-22.8	8156 - 8016	8171 - 7995	4 / 5	*Caryx* cf. (2 seeds)
MWP_09	OxA-32206	114	9230 ± 40	-26.6	10480 - 10290	10506 - 10257	4 / 5	*Potentilla* sp., Rumex sp,
MWP_23	OxA-X-2623-15 †*	149	1.03763 ± 0.00595	-25.6	*	*	(100 / 5) *	Unidentifiable terrestrial plants
MWP_10	OxA-31358	157	10635 ± 50	-26.6	12668 - 12573	12715 - 12447	4 / 5	Unidentifiable terrestrial plants
Spring Lake								
MWP_11	OxA-X-2623-11 †	70	3465 ± 65	-22.8	3829 - 3643	3901 - 3568	4 / 5	*Picea* cf. *mariana*
MWP_35	OxA-31898	180.5	7248 ± 35	-10.8	8158 - 8014	8170 - 7992	4 / 5	Grass (two ears)
MWP_15	OxA-31587	233	10010 ± 45	-27.1	11604 - 11331	11707 - 11145	3 / 5	Unidentifiable terrestrial plants
MWP_15	OxA-31588	233	10040 ± 45	-28.7	11604 - 11331	11707 - 11145	3 / 5	Unidentifiable terrestrial plants
MWP_16	OxA-31589	250	10045 ± 45	-26.8	11701 - 11556	11746 - 11483	3 / 5	Unidentifiable terrestrial plants
MWP_02	OxA-31586	262	10175 ± 45	-27.8	11735 - 11616	11825 - 11510	6 / 5	Unidentifiable terrestrial plants
MWP_17	OxA-31590	273	10105 ± 45	-26.1	11762 - 11649	11905 - 11615	3 / 5	Unidentifiable terrestrial plants
MWP_18	OxA-31355	278	10080 ± 55	-24.6	11791 - 11662	11925 - 11624	4 / 5	*Sphagnaceae*, cf. *Sphagnum*
MWP_03	OxA-31354	288	10105 ± 50	-25.4	11836 - 11673	11978 - 11641	4 / 5	Unidentifiable terrestrial plants

Data were calibrated with the IntCal13 calibration curve[59] and modelled using the Bayesian statistical software OxCal v. 4.2 (refs. 60, 61, 73).
†Samples that represent 'very small graphite' AMS targets (<0.5 mg C), and so should be treated with caution (and hence the 'OxA-X-' laboratory code prefix).
*Three samples from Charlie Lake produced statistically outlying dates (>50% probability) that were excluded from the final age model.